Received: 15 June 2018 | Accepted: 25 August 2018

DOI: 10.1002/pamm.201800237

Modelling and Finite Element Analysis of Viscoelastic Adhesive Joints

Thomas Rehbein[1,*] and **Anton Matzenmiller**[1]

[1] Institute of Mechanics, Department of Mechanical Engineering, University of Kassel, Mönchebergstraße 7, 34125 Kassel, Germany

Besides large nonlinear deformations, polyurethane adhesives exhibit elastic and viscous material behaviour simultaneously. Although the concept of rheological elements is a quite simple method to describe rate effects, the identification of model parameters is a challenging task. Dynamic mechanical analysis provides the experimental database. By using time-temperature superposition, the experimental frequency range can be extended in order to identify the relaxation times and dimensionless stiffnesses of the rheological network. The simulation results are in good agreement with stress-strain curves from tests with different strain rates.

© 2018 Wiley-VCH Verlag GmbH & Co. KGaA, Weinheim

1 Constitutive model for polyurethane adhesives

The thick polyurethane adhesive layer with a thickness of 5 mm is modelled by a three-dimensional finite viscoelasticity model with respect to the reference configuration. Due to its nearly incompressibility, the second PIOLA-KIRCHHOFF stress is split into a volumetric and isochoric part additively over time t, whereby the volumetric part exhibits no viscous effects, see [1].

$$\tilde{\mathbf{T}}(t) = \tilde{\mathbf{T}}_{\text{vol}}(t) + \tilde{\mathbf{T}}_{\text{iso}}(t) \quad , \quad \tilde{\mathbf{T}}_{\text{vol}}(t) = J\frac{\mathrm{d}U}{\mathrm{d}J}\mathbf{C}^{-1}(t) \tag{1}$$

$$\tilde{\mathbf{T}}_{\text{iso}}(t) = \int\limits_{-\infty}^{t} \left(\gamma_\infty + \sum_{i=1}^{N}\gamma_i \exp\left(-\frac{t-s}{\tau_i}\right)\right)\frac{\mathrm{d}}{\mathrm{d}s}\left(2\left(\frac{\mathrm{d}\bar{\mathbf{C}}}{\mathrm{d}\mathbf{C}}\right)^{\top} : \frac{\mathrm{d}\bar{W}^0\left(I_{\bar{\mathbf{C}}}, I\!I_{\bar{\mathbf{C}}}\right)}{\mathrm{d}\bar{\mathbf{C}}}\right)\mathrm{d}s \tag{2}$$

In the isochoric part, the generalised MAXWELL solid consisting of N parallel chains with springs and dashpots is used with relaxation times $\tau_1, \ldots, \tau_{\text{N}}$ and dimensionless stiffnesses $\gamma_1, \ldots, \gamma_{\text{N}}$, respectively. For quasi-static processes, the isochoric model response is governed by the dimensionless equilibrium stiffness γ_∞ only. The purely elastic bulk behaviour is described by a model proposed by MIEHE (see [2]) depending on the Jacobian J and bulk modulus K, whereas the instantaneous, isochoric response is defined by the MOONEY-RIVLIN model which has two model parameters C_{10} and C_{01} as well as depends on the first and second invariant of the unimodular right CAUCHY-GREEN tensor $\bar{\mathbf{C}} = J^{-2/3}\mathbf{C}$ (see [4], p. 100).

$$U(J) = K(J - \ln J - 1) \quad , \quad \bar{W}^0\left(I_{\bar{\mathbf{C}}}, I\!I_{\bar{\mathbf{C}}}\right) = \frac{C_{10}}{2}\left(I_{\bar{\mathbf{C}}} - 3\right) + \frac{C_{01}}{2}\left(I\!I_{\bar{\mathbf{C}}} - 3\right) \tag{3}$$

Thus, the proposed model has $2N + 4$ parameters in total. The push-forward operations for the CAUCHY stress and the spatial tangent modulus in terms of the deformation gradient $\mathbf{F}$ provide the required expressions for the implementation into the commercial finite element program LS-DYNA.

$$\boldsymbol{\sigma}(t) = J^{-1}\mathbf{F}\tilde{\mathbf{T}}(t)\mathbf{F}^{\top} \quad , \quad \boldsymbol{\mathcal{C}} = J^{-1}\left[\mathbf{F}\otimes\mathbf{F}\right]^{\top_{23}} : \Big(2\,\mathrm{d}\tilde{\mathbf{T}}(t)/\mathrm{d}\mathbf{C}(t)\Big) : \left[\mathbf{F}^{\top}\otimes\mathbf{F}^{\top}\right]^{\top_{23}} \tag{4}$$

The dimensionless stiffnesses and relaxation times are assumed to be constant through the deformation process. Hence, the identification of parameters for the viscous behaviour is carried out in the domain of small deformations as proposed in [3].

2 Parameter identification

The identification of the model parameters is split into two consecutive steps: at first, the relaxation times $\tau_1, \ldots, \tau_{\text{N}}$ and dimensionless stiffnesses $\gamma_\infty, \gamma_1, \ldots, \gamma_{\text{N}}$ of the generalised MAXWELL solid are identified simultaneously by means of test data from dynamic mechanical analysis . For this purpose, the mastercurve of the storage modulus E' is created at room temperature. The viscoelastic modelling of the rectangular adhesive bar clamped at both ends and loaded by harmonic excitation $u(t) = \hat{u}\sin(\omega t)$ with varying angular frequency ω and small displacement amplitude $\hat{u} = 40\ \mu$m leads to the analytical relation between storage modulus and spring stiffnesses $E_\infty, E_1, \ldots, E_{\text{N}}$ as well as relaxation times of the generalised MAXWELL solid (see eq. $(5)_1$).

$$E' = E_\infty + \sum_{i=1}^{N} E_i \frac{(\omega\tau_i)^2}{1 + (\omega\tau_i)^2} \quad , \quad E^0 = E_\infty + \sum_{i=1}^{N} E_i \quad , \quad \gamma_\infty = E_\infty/E^0 \quad , \quad \gamma_i = E_i/E^0 \tag{5}$$

* Corresponding author: e-mail thomas.rehbein@uni-kassel.de, phone +49 561 804 2058, fax +49 561 804 2720

The dimensionless stiffnesses $\gamma_\infty, \gamma_1, \ldots, \gamma_\mathrm{N}$ are calculated based on the expressions in eqs. $(5)_{2\text{-}4}$. In order to extend the experimental frequency range, time-temperature superpositon is applied resulting in a large shifted frequency range of 20 decades. The identification process is carried out by the commercial program LS-OPT using a gradient based optimisation procedure. Additionally, the sophisticated error measure MSLE is applied causing no penalisation of differences between either low or high predicted values $E'_{i,\mathrm{sim}}$ and target values $E'_{i,\mathrm{exp}}$.

$$\mathrm{MSLE} = \frac{1}{R}\sum_{i=1}^{R}\left[\log\left(E'_{i,\mathrm{sim}}(\boldsymbol{x})\right) - \log\left(E'_{i,\mathrm{exp}}\right)\right]^2 \tag{6}$$

The vector $\boldsymbol{x}$ and scalar value R denote the design space vector, i.e. relaxation times and dimensionless stiffnesses, and number of regression points, respectively. Fig. 1 shows the isothermal curves of the storage modulus E' and the manually created mastercurve (Exp.) with the simulation result (Sim.) at room temperature. The shifted frequency range is divided into 20 equidistantly distributed sections in logarithmic scale. Thus, one MAXWELL chain is used for each decade leading to the simultaneous identification of 41 parameters in total.

After completing the determination of the parameters for the viscous behaviour, the parameters K, C_{10} and C_{01} are identified by means of test data from the thick adherend shear specimen (TASS) and butt joint specimen (BJS) (red dots in Fig. 2). Moreover, the BJS with a thinner adhesive layer thickness of 2 mm is used to determine the bulk modulus. As a result, only four different experimental setups are needed to identify all model parameters.

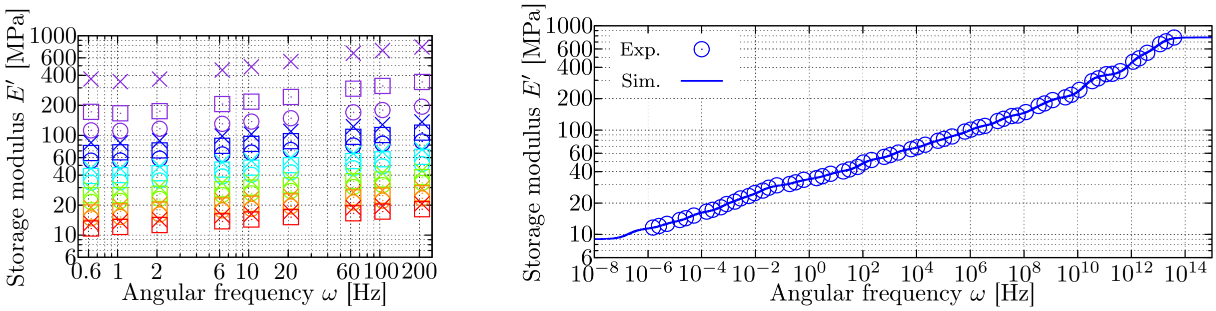

Fig. 1: Isothermal curves of the storage modulus E' (left) from [5], p. 15, and shifted mastercurve (Exp.) with simulation result (Sim.) at room temperature (right).

3 Validation

To demonstrate the quality of the constitutive model and identified model parameters, stress-strain curves from three-dimensional finite element simulations are compared to test data of the TASS and BJS (see [6]) loaded by variable strain rates. The strain rates range from $\dot{\gamma} = 0.01 \ldots 100\ \mathrm{s}^{-1}$ for the TASS and $\dot{\varepsilon} = 0.005 \ldots 50\ \mathrm{s}^{-1}$ for the BJS, respectively. The computed stress-strain curves (solid lines) are in good agreement with the test data (points) - see Fig. 2.

Further investigations include the consideration of different failure phenomena, such as cavitation and visible cracks, which initiate far below the ultimate strength of the adhesive joint.

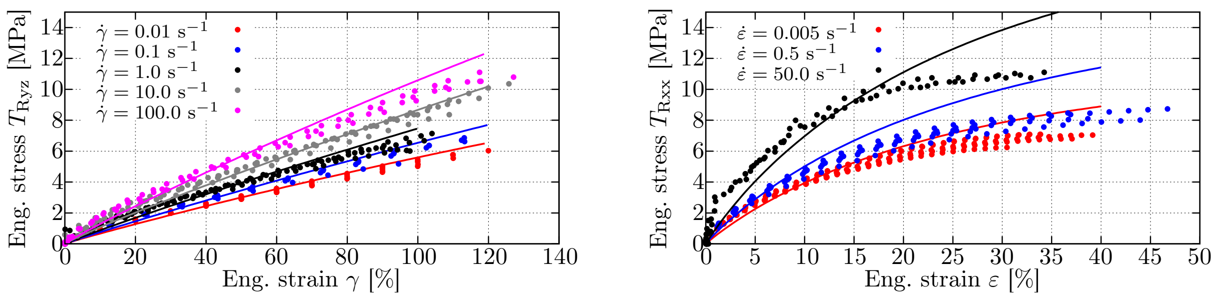

Fig. 2: Validation for the TASS (left) and BJS (right) with adhesive layer thickness of 5 mm loaded by different strain rates.

References

[1] J. C. Simo and T. J. R. Hughes, Computational Inelasticity (Springer-Verlag, New York, 1998), p. 366.
[2] C. Miehe, Int. J. Numer. Methods Eng. **37**, 1981-2004 (1994).
[3] P. Haupt, A. Lion and E. Backhaus, Int. J. Solids Struct. **37**, 3633-3646 (2000).
[4] A. Nelson and A. Matzenmiller, in: Numerical modelling and experimental characterization for the failure behaviour of hyperelastic adhesives, FOSTA-Report P 1086 (Verlag und Vertriebsgesellschaft mbH, Sohnstr. 65, 40237 Düsseldorf, 2017, in press), pp. 99-106.
[5] G. Schwarzkopf and G. Meschut, in: Numerical modelling and experimental characterization for the failure behaviour of hyperelastic adhesives, FOSTA-Report P 1086 (Verlag und Vertriebsgesellschaft mbH, Sohnstr. 65, 40237 Düsseldorf, 2017, in press), pp. 13-16.
[6] G. Schwarzkopf, Laboratory for Materials and Joining Technology (LWF), Paderborn University, private communication.

© 2018 Wiley-VCH Verlag GmbH & Co. KGaA, Weinheim